Experimental Study of the Dry and Near-Dry Electrical Discharge Milling Processes

Jia Tao

Albert J. Shih[1]
e-mail: shiha@umich.edu

Jun Ni

Mechanical Engineering,
University of Michigan,
Ann Arbor, MI 48109-2125

This study investigates the dry and near-dry electrical discharge machining (EDM) milling to achieve a high material removal rate (MRR) and fine surface finish for roughing and finishing operations, respectively. Dry EDM uses gas and near-dry EDM applies a liquid-gas mixture as the dielectric medium. Experimental studies leading to the selection of oxygen gas and copper electrode for high MRR dry EDM and the nitrogen-water mixture and graphite electrode for fine surface finish near-dry EDM are presented. Near-dry EDM exhibits the advantage of good machining stability and surface finish under low discharge energy input. A 2^{5-1} fractional factorial design is applied to investigate the effect of discharge current, pulse duration, and pulse interval on the MRR and surface finish in dry and near-dry EDMs. Lower pulse duration and lower discharge current are identified as key factors for improving the surface finish in near-dry EDM.
[DOI: 10.1115/1.2784276]

1 Introduction

Dry and near-dry electrical discharge machining (EDM) processes use gas and liquid-gas mixture, respectively, as a dielectric medium to substitute the liquid dielectrics in a conventional EDM. The dry EDM was first reported in a short NASA technical note [1] in 1985 for hole drilling using argon or helium gas as a dielectric medium. The research group led by Kunieda et al. [2–4] has extensively studied the feasibility and capability of dry EDM. Using oxygen as the dielectric medium, a very high material removal rate (MRR) can be achieved in dry EDM under the so-called "quasiexplosion" mode [4]. However, in shop floor production environment, dry EDM has several shortcomings, such as low MRR using non-oxygen gas, debris reattachment, and odor of burning [5].

The feasibility of near-dry EDM was explored by Tanimura et al. [6], who investigated EDM in water mists with air, nitrogen, and argon gases. Further investigation of near-dry EDM was conducted by Kao et al. [7] in wire EDM experiments. Advantages of near-dry EDM were identified as a stable machining process at low discharge energy input because the presence of liquid phase in the gas environment changes the electric field, making discharge easier to initiate and thus creating a larger gap distance. In addition, good machined surface integrity without debris reattachment that occurred in dry EDM was attained since the liquid in the dielectric fluid enhances debris flushing. Other potential advantages of near-dry EDM are a broad selection of gases and liquids and flexibility to adjust the concentration of the liquid in gas. The dielectric properties can thus be tailored in near-dry EDM to meet various machining needs, such as high MRR or fine surface finish. The technical barrier in dry and near-dry EDMs lies in the selection of proper dielectric medium and process parameters. To overcome this barrier, it becomes the goal of this research to explore the process capability and parameter selection of the dry and near-dry EDM processes through experimental studies.

The dielectric fluid and its delivery method are critical to the performance of EDM. The electrical, mechanical, and thermal properties of the dielectric fluid influence the processes of discharge initiation, plasma expansion, material erosion, debris removal, and discharge channel reconditioning in EDM [8]. Table 1 summarizes key properties of the gas and liquid as EDM dielectric fluids [9–16]. Properties of the liquid-gas mixture are expected to lie in between the properties of the base materials.

The dielectric strength determines the gap distance between the electrode and workpiece. Higher dielectric strength requires higher electric field to break down the dielectric fluid and thus decrease the gap distance. Liquid dielectric media have higher dielectric strength (>10 MV/m) than that of gas dielectric media (<4 MV/m). The dielectric constant determines the stray capacitance induced by the overlapping area between the electrode and workpiece. Larger dielectric constant induces larger stray capacitance and requires higher minimum discharge energy [17]. The large inertia and viscosity of the fluid increase the bubble expansion force and material removal per discharge [18]. The larger inertia and higher viscosity of the liquid dielectric indicate a faster MRR but a rougher surface finish. Heat conductivity and heat capacity are important factors that affect the solidification of molten debris and the cooling of the electrode and the workpiece surfaces [19]. In Table 1, the liquid dielectric fluids have the thermal conductivity and heat capacity at least ten times and twice that of gas dielectric fluids (except for He, which has exceptionally high heat capacity). A wide range of dielectric properties can be obtained by using different compositions and properties of the dielectric media, and dry and near-dry EDMs will thus yield a diverse range of performance compared with conventional wet EDM. This study investigates the selection of dry and near-dry EDM process setup and parameters to achieve two distinctly different performance goals: the high MRR for roughing operations and the fine surface finish EDM finishing operations.

In this paper, the experimental setup and design for dry and near-dry EDMs are first presented. The selection of dielectric medium and electrode material, exploratory experiments to determine the setup for the external air jet, depth of cut, gas input pressure, discharge current and pulse duration, and two detailed designs of experiments (DOEs) for dry and near-dry EDMs are discussed.

[1]Corresponding author.

Contributed by the Manufacturing Engineering Division of ASME for publication in the JOURNAL OF MANUFACTURING SCIENCE AND ENGINEERING. Manuscript received June 7, 2007; final manuscript received August 10, 2007; published online January 16, 2008. Review conducted by Bin Wei.

Table 1 Electrical, thermal, and mechanical properties of liquid and gas dielectric media at room temperature [8–15]

	Liquid		Gas			
	De-ionized water	Kerosene/ hydrocarbon oil	Air	N_2	O_2	He
Dielectric strength (MV/m)	13	14 to 22	3	2.8	2.6	1.2
Dielectric constant	80.4	1.8	1.000536	1.00058	1.00049	1.055
Dynamic viscosity (g/m s)	0.92	1.64	0.019	0.017	0.020	0.020
Thermal conductivity (W/m K)	0.606	0.149	0.026	0.0254	0.026	0.015
Heat capacity (J/g K)	4.19	2.16	1.04	1.04	0.92	5.19

2 Experimental Setup and Design

2.1 Experimental Setup. The dry and near-dry EDM milling experiments were conducted on a Vanguard 150H computer numerical control (CNC) die-sinking EDM machine from EDM Solutions. A rotary spindle, Rotobore RBS-1000, with through-spindle flushing capability is used to hold the tubular electrode. Figure 1(*a*) shows the setup of the spindle, tool electrode, and dielectric medium inlet. The spindle rotates the tool electrode to maintain the uniform tool wear and enhance the debris removal.

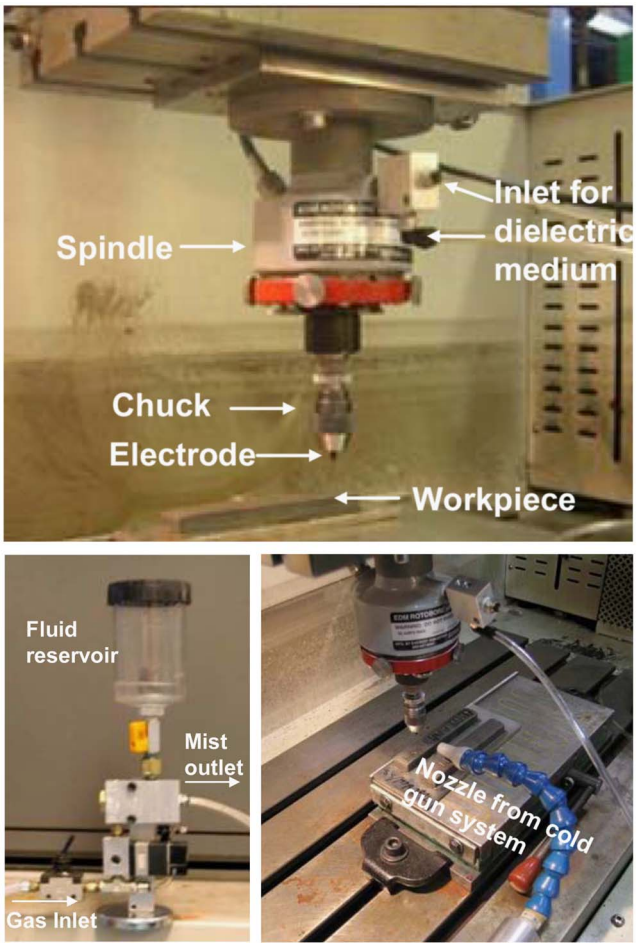

Fig. 1 Dry and near-dry EDM experimental setup: (*a*) rotary spindle and electrode, (*b*) spray delivery device, and (*c*) nozzle to deliver cold air

The dielectric fluid, which can be in the form of liquid, gas, or liquid-gas mixture, is delivered through a tubular tool electrode. The liquid-gas mixture is generated by an AMCOL 6000 pulsed spray generator, as shown in Fig. 1(*b*), designed for minimum quantity lubrication (MQL) machining applications. In this study, the input liquid flow rate was fixed at 5 ml/min. Figure 1(*c*) shows the setup of a nozzle to deliver a chilled air jet (around –3 °C) from an Exair model 5215 cold gun system. The external air jet helps to solidify and flush away the molten debris. This is especially useful in a roughing operation when a large amount of molten debris is generated due to high discharge energy.

The experimental process variables and settings are summarized in Table 2. Copper and graphite are two electrode materials evaluated. The tubular electrode is 3 mm in outer diameter and 1.5 mm and 1 mm in inner diameter for copper and graphite electrode, respectively. For liquid dielectric, de-ionized water and kerosene are selected. The liquid dielectric is mixed with four types of gas: air, oxygen, nitrogen, and helium in near-dry EDM. Oxygen is expected to yield high MRR due to the exothermic chemical reaction that occurs [4]; air is a readily available gas; helium has very high heat capacity and is an inert gas that can prevent oxidation; and nitrogen can potentially form a hard nitride layer on a steel workpiece surface to improve the wear resistance [20]. The kerosene-oxygen mixture is excluded from the investigation because of fire and explosion risks [21]. The dielectric fluid pressure is closely related to the discharge environment, such as debris concentration and fluid viscosity, and hence was investigated at different pressure levels.

The depth of cut for the finishing operation was set at 0.02 mm and varied between 0.1 mm and 0.6 mm in the roughing operation to achieve a higher MRR. The electrode rotary speed was fixed at 250 rpm since no obvious influence was observed at higher rotary speed.

The electrical parameters are among the most important factors in EDM. The discharge current (i_e), pulse duration (t_i) and gap voltage (u_e) determine the discharge energy per pulse; the pulse interval (t_0) decides the time available for gap reconditioning between two consecutive discharges; the open circuit voltage (u_i) controls the discharge gap distance; and the polarity influences the material removal ratio between the electrode and workpiece. In this study, different levels of these electrical parameters are selected to study both the roughing and finishing, and dry and near-dry EDM processes.

2.2 Experimental Procedures. Figure 2 illustrates the configuration of the EDM milling process. Grooves of 8 mm in length and varied depth for different processes were made. To measure the surface roughness at the bottom of the slot, a Taylor Hobson Form Talysurf profilometer with a 2 μm stylus radius was used. The cutoff length was set to 0.25 mm for the finished surface and 0.8 mm for the roughened surface. The measurement length was set to 8 mm. The weight of the part before and after

Table 2 Process parameters for dry and near-dry EDM experiments

Machining media	Electrode material		Copper, graphite
	Dielectric fluid	Liquid	De-ionized water, hydrocarbon oil (kerosene)
		Gas	Oxygen, air, nitrogen, helium
		Liquid-gas mixture	Water with oxygen, air, nitrogen, or helium; kerosene with air, nitrogen, or helium
Machining parameters	Pressure of the dielectric fluid (kPa)		276, 413, 483, 552, 621
	Depth of cut (mm)		0.02 for finishing; 0.1–0.6 for roughing
	Electrode diameter (mm)		3
	Electrode rotary speed (rpm)		250
Electrical parameters	Discharge current (A)		1, 2, 3, 20, 25, 30, 40
	Pulse duration (μs)		2, 4, 8, 12
	Pulse interval (μs)		4, 8, 16, 20, 40
	Gap voltage (V)		160, 210, 260
	Open circuit voltage (V)		40, 60, 80
	Polarity		Electrode negative

machining was measured using an Ohaus GA110 electronic scale with a 0.1 mg resolution and converted to the volumetric material removal and MRR.

The experimental investigation of dry and near-dry EDMs was carried out in three sets of experiments, marked as Expts. I, II, and III.

1. Expt. I. Dielectric medium and electrode material selection: Experiments were conducted to select the dielectric medium and electrode material at high and low discharge energy levels for roughing and finishing operations, respectively. The depth of cut and the input pressure were set at 0.1 mm and 480 kPa, respectively, for the roughing operation and at 0.02 mm and 480 kPa, respectively, for the finishing operation.
2. Expt. II. Exploratory experiments: Based on the selected dielectric medium and electrode material, several sets of experiments were conducted to investigate the effects of external air jet, depth of cut, gas input pressure, discharge current, and pulse duration in dry EDM roughing and near-dry EDM finishing.
3. Expt. III. DOE: Two DOE tests based on the 2^{5-1} fractional factorial design were performed to study the effect of five process parameters (i_e, t_i, u_e, t_0, and u_i) and their interactions. Four center points were used in the design to test the curvature effect of the model. The design matrices are listed in Table 3. Analysis of variance (ANOVA) was applied to analyze the main effects and interactions [22–24] of input parameters. The DOE results can identify directions for further process optimization.

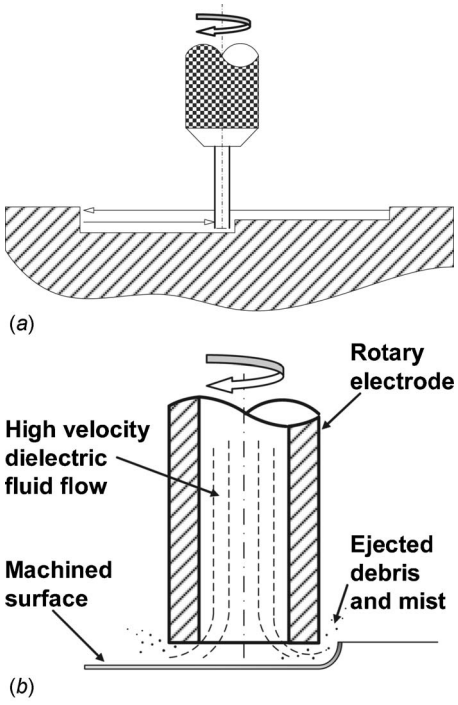

Fig. 2 Configuration of EDM milling: (*a*) Overview and (*b*) close-up view of the electrode and cutting region

3 Experiment I Results: Electrode Material and Dielectric Medium

Experiments were conducted at high and low discharge energies to study effects of the electrode material and dielectric medium for roughing and finishing operations, respectively. Figure 3(*a*) shows the results on MRR and surface roughness at high discharge energy input. The copper electrode was successful at removing the work-material in nearly all dry and near-dry EDM cases (except the near-dry EDM with kerosene-nitrogen and kerosene-helium mixtures). However, the graphite electrode failed in a high discharge energy setting due to severe arcing. The de-

Table 3 Roughing and finishing DOE

Roughing process experiments						Finishing process experiments					
Run	t_i (μs)	i_e (A)	u_i (V)	u_e (V)	t_0 (μs)	Run	t_i (μs)	i_e (A)	u_i (V)	u_e (V)	t_0 (μs)
1	4	20	160	40	20	1	2	1	160	80	12
2	12	20	160	40	8	2	4	1	160	40	4
3	4	30	160	40	8	3	2	3	160	40	12
4	12	30	160	40	20	4	4	3	160	80	4
5	4	20	260	40	8	5	2	1	260	80	4
6	12	20	260	40	20	6	4	1	260	40	12
7	4	30	260	40	20	7	2	3	260	40	4
8	12	30	260	40	8	8	4	3	260	80	12
9	4	20	160	80	8	9	4	3	260	40	4
10	12	20	160	80	20	10	2	3	260	80	12
11	4	30	160	80	20	11	4	1	260	80	4
12	12	30	160	80	8	12	2	1	260	40	12
13	4	20	260	80	20	13	4	3	160	40	12
14	12	20	260	80	8	14	2	3	160	80	4
15	4	30	260	80	8	15	4	1	160	80	12
16	12	30	260	80	20	16	2	1	160	40	4
17	8	25	210	60	14	17	3	2	210	60	8
18	8	25	210	60	14	18	3	2	210	60	8
19	8	25	210	60	14	19	3	2	210	60	8
20	8	25	210	60	14	20	3	2	210	60	8

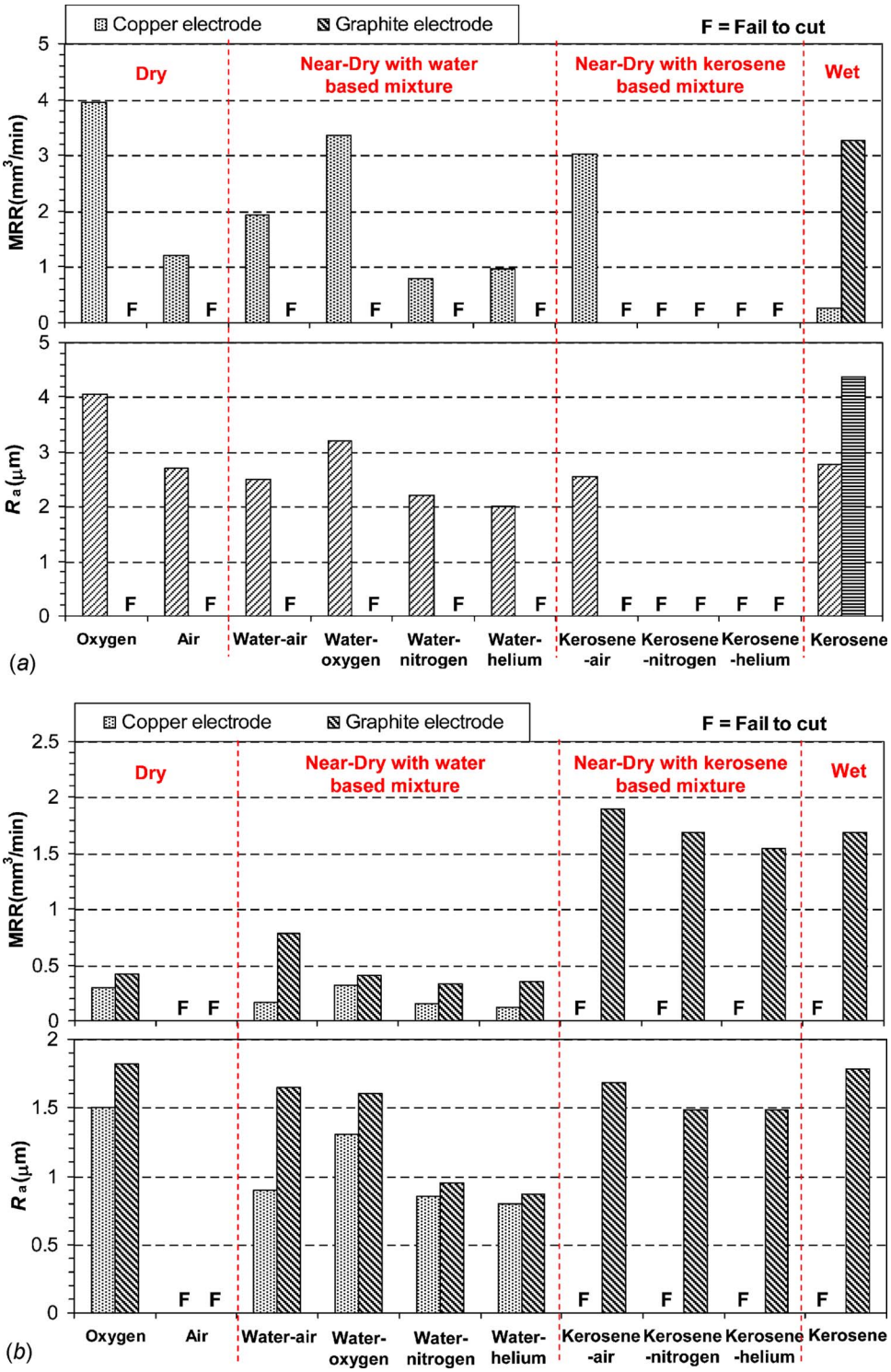

Fig. 3 MRR and R_a results of different dielectric fluids for copper and graphite electrode materials: (*a*) at high discharge energy input (i_e=20 A, t_i=4 μs, t_0=8 μs, u_e=60 V, and u_i=200 V) and (*b*) at low discharge energy input (i_e=1 A, t_i=4 μs, t_0=8 μs, u_e=60 V, and u_i=200 V)

posited workpiece material, similar to that in arc welding, was observed at the outer circumference of the machined spot, as shown in Fig. 4(*a*). The severe arcing causes discharge localization and large scale material melting, while ideal sparks should uniformly distribute over the machining area and erode the material. The arcing was likely stimulated by the excessive amount of graphite powder chipped off from the electrode tip, as shown in Fig. 4(*b*). The high thermal load, due to lower cooling efficiency in dry and near-dry EDMs, cracked the brittle graphite electrode. The resultant graphite powder bridged the workpiece and electrode, causing discharge localization and, thus, arcing.

For the effect of dielectric medium, oxygen, water-oxygen mixture, and kerosene-air mixture are found to achieve comparable MRRs and better surface finish than liquid kerosene in wet EDM.

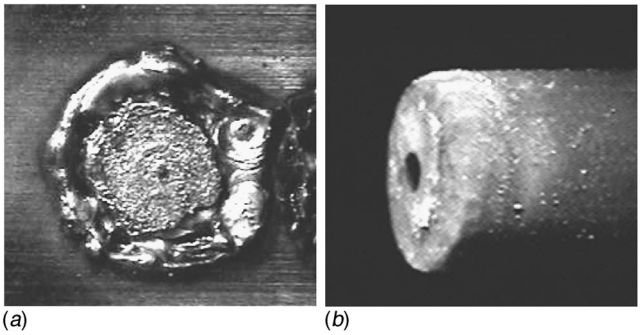

(*a*) (*b*)

Fig. 4 Graphite electrode in near-dry EDM at high discharge current: (*a*) Damaged workpiece surface due to arcing and (*b*) damage tool (i_e=20 A, t_i=4 μs, t_0=8 μs, u_e=60 V, and u_i =200 V)

The lower viscosity of the liquid-gas mixture resulted in shallower craters on the machined surface and, thus, better surface finish.

Since oxygen was confirmed to have the highest MRR, its potential is further exploited in this study. Water-oxygen mixture is another good candidate for roughing since it provided high MRR close to that of oxygen and had good surface finish. The flushing of water-oxygen mixture is helpful in high discharge energy to solidify and remove the molten debris. However, the water combined with oxygen induces severe electrolysis corrosion on a machined surface. Hence, copper electrode and oxygen gas are selected for further DOE study of high MRR roughing EDM.

Figure 3(*b*) shows the results of the MRR and surface roughness at low discharge energy input. The graphite electrode exhibited its advantage over copper electrode with higher MRR and comparable surface roughness. In near-dry EDM using water mixture with nitrogen or helium, the graphite electrode achieved a similar quality of the surface finish (0.87–0.95 μm R_a) and twice the MRR as that of copper electrode. At low discharge energy input, the graphite powder, which exists in much smaller amounts than that at high discharge energy, assisted the machining process to improve the discharge transitivity [25] and, consequently, the MRR. It is hypothesized that the carbon powder plays a role in assisting the discharge ignition and evenly distribute the sparks, as identified by Yang and Cao [17].

The copper electrode produced slightly better surface finish, 0.80 μm and 0.85 μm R_a, using water-helium and water-nitrogen mixtures, respectively, but its MRR was low compared with graphite. The frequent servo retraction was observed when using the copper electrode at low discharge energy, probably because the discharge is difficult to initiate. When kerosene or kerosene based mixtures were used as dielectric fluids, the copper electrode cannot maintain stable discharges because of the narrow gap distance in the low discharge energy EDM [26].

Considering the effect of the dielectric medium, near-dry EDM outperformed both dry and wet EDMs to generate better surface finish and higher MRR. The best surface finish of 0.8 μm was achieved using the water-nitrogen mixture. The highest MRR of 1.8 mm^3/min was obtained using the kerosene-air mixture. In dry EDM at low energy input, the MRR was low, using an oxygen medium, and the surface was rough.

The water based mixture generally provided better surface finish than the kerosene based mixture with the sacrifice of MRR due to its lower viscosity and correspondingly smoother and shallower crater for each discharge. Water-nitrogen and water-helium mixtures yielded better surface finishes (0.95 μm and 0.87 μm R_a for graphite electrode and 0.85 μm and 0.80 μm R_a for copper electrode) than the water-air and water-oxygen mixtures (1.68 μm and 1.62 μm R_a for graphite electrode and 0.98 μm and 1.25 μm R_a for copper electrode). A possible reason is that nitrogen and helium shielded the process from oxygen and thus reduce the corrosion caused by water electrolysis. The mixture with helium produced a slightly better surface finish over that of nitrogen. Nitrogen has the potential to form a hard nitride surface layer by alloying with elements in the work-material [20].

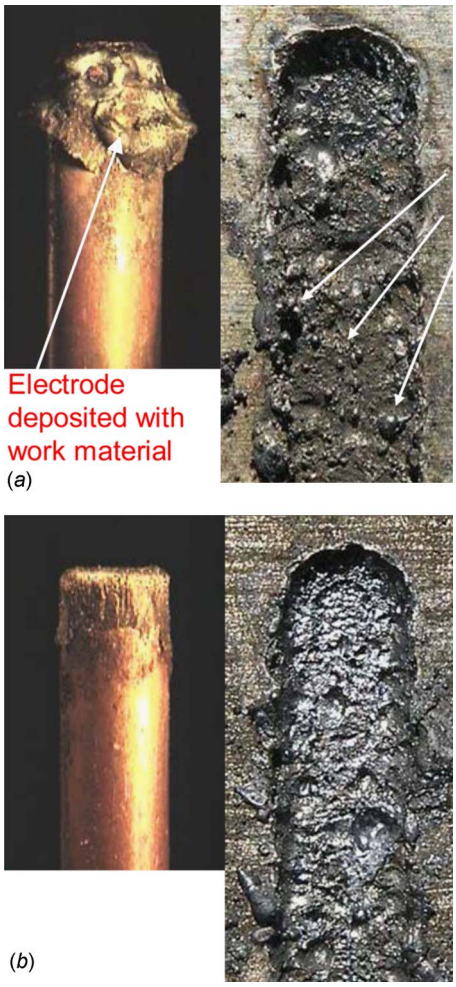

Fig. 5 Worn electrode and grooves milled using oxygen as a dielectric fluid (i_e=20 A, t_i=4 μs, t_0=8 μs, u_e=60 V, and u_i =200 V): (*a*) Without using cold gun (R_a=14.2 μm; MRR =20 mm^3/min) and (*b*) using cold gun (R_a=13.2 μm; MRR =22 mm^3/min)

Kerosene-air mixture produced higher MRR than that of kerosene with nitrogen or helium. The oxygen content in the air generates more heat for material removal through an exothermic re-

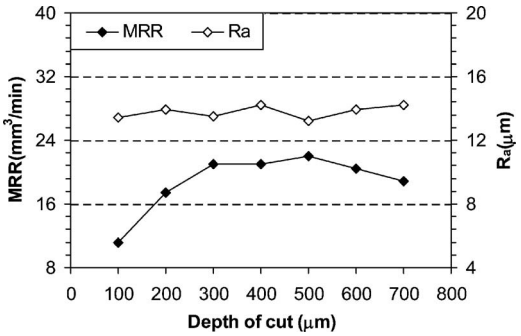

Fig. 6 Effect of the depth of cut on dry EDM rough cutting with oxygen (i_e=30 A, t_i=4 μs, t_0=8 μs, u_e=60 V, and u_i=200 V)

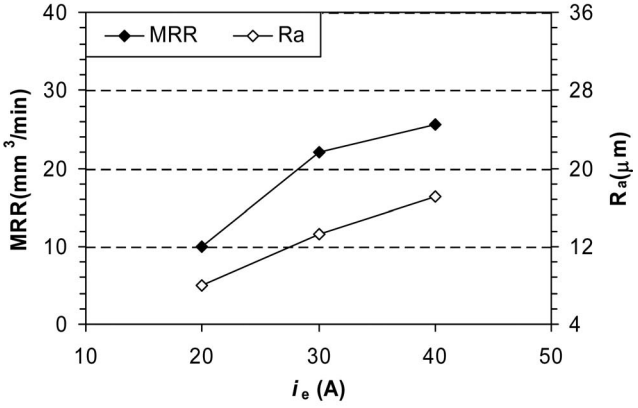

Fig. 7 Effect of the discharge current on high energy input dry EDM with oxygen (t_i=4 μs, t_0=8 μs, u_e=60 V, and u_i=200 V)

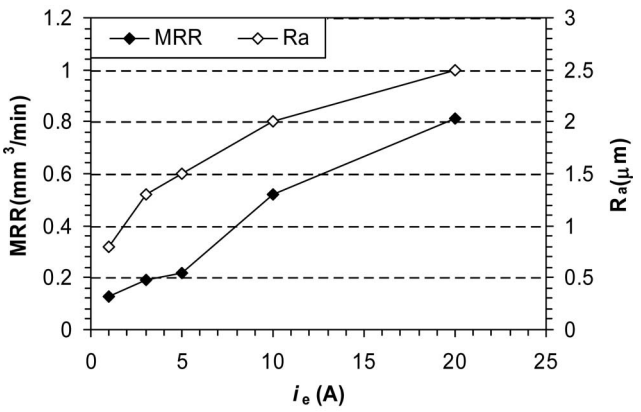

Fig. 8 Effect of the discharge current on the finishing EDM (t_i=4 μs, t_0=8 μs, u_e=60 V, and u_i=200 V, copper electrode)

action [20], but the surface finish was adversely affected. When kerosene was used as dielectric media, the deterioration caused by electrolysis corrosion was not observed [27].

For further DOE study of finishing EDM, the graphite electrode and water-nitrogen mixture are selected. Nitrogen is selected over helium because of the comparable performance, lower cost, and potential to form a hard nitride surface layer on the machined surface for better wear resistance.

4 Experiment II Results: Selection of External Air Jet, Depth of Cut, Discharge Current, and Gas Inlet Pressure

The application of the external air jet and the selection of the depth of cut, discharge current, and gas inlet pressure were investigated to further understand the high MRR dry EDM and fine surface finish near-dry EDM processes.

4.1 External Air Jet. Blowing an air jet outside the EDM region can improve the surface quality in roughing EDM, where high discharge energy generates a large amount of molten debris. Flushing simply by the gas flowing through the tubular electrode is not enough to remove the molten debris. As observed in Fig. 5(*a*), spherical debris droplets resolidified to the machined surface and deteriorated the surface quality. The tool electrode also had the same problem of debris deposition. By externally blowing high flow rate air, the molten debris was better solidified and flushed away. As a result, the surface finish was improved and the shape of the electrode was maintained better, as shown in Fig. 5(*b*). In addition, arcing frequency was greatly reduced due to the improved discharge gap conditioning. The surface finish, R_a, was improved from 14.2 μm to 13.2 μm and the MRR was increased from 20 mm^3/min to 22 mm^3, with the assistance of external air jet close to the EDM region. All DOE roughing EDM experiments were carried out with the air jet assisted debris flushing.

4.2 Depth of Cut. Figure 6 shows the effect of the depth of cut in oxygen assisted dry EDM roughing. The MRR reached the maximum, 22 mm^3/min, at a 500 μm depth of cut. When the depth of cut is beyond 500 μm, the increase of MRR is limited due to the debris removal problem. The debris can bridge between the electrode sidewall and workpiece, resulting in arcing or short circuit. This was confirmed by observing frequent servo retraction of the electrode to regulate the discharge condition. The surface roughness was generally not affected by the depth of cut because it does not influence the discharge condition at the bottom of the electrode. In the following DOE roughing experiments with oxygen, the depth of cut was set at 500 μm.

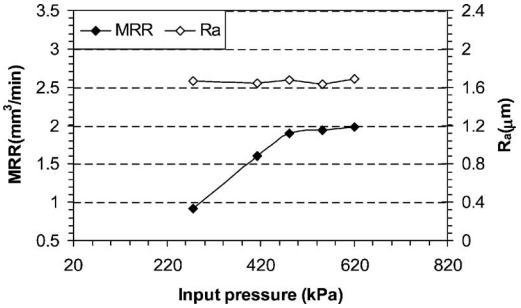

Fig. 9 Effect of the input pressure of the spray delivery device to the finishing process (i_e=1 A, t_i=2 μs, t_0=16 μs, u_e=20 V, and u_i=200 V, graphite electrode with kerosene-air mixture)

4.3 Discharge Current. Figure 7 shows the effect of discharge current, i_e, in the roughing operation. Higher discharge current increases the discharge energy, removes more work material, and generates a rougher surface. The increase of MRR and surface roughness with i_e is significant. Experiments with higher i_e was limited due to the maximum current limit of the rotary spindle.

Figure 8 shows the effect of discharge current using water-nitrogen mixture in near-dry EDM finishing. The surface finish

Table 4 MRR and R_a results for roughing DOE

Run	1	2	3	4	5	6	7	8	9	10
MRR (mm^3/min)	1.14	7.89	26.04	3.23	3.26	2.19	2.21	50.0	2.95	2.74
R_a (μm)	4.37	4.32	17.94	3.82	3.66	3.67	4.47	20.2	4.35	3.99
Run	11	12	13	14	15	16	17	18	19	20
MRR (mm^3/min)	2.43	36.04	1.20	12.5	28.2	6.10	5.76	5.90	5.93	5.29
R_a (μm)	5.01	18.75	6.13	4.15	17.34	4.52	5.58	5.98	5.31	5.68

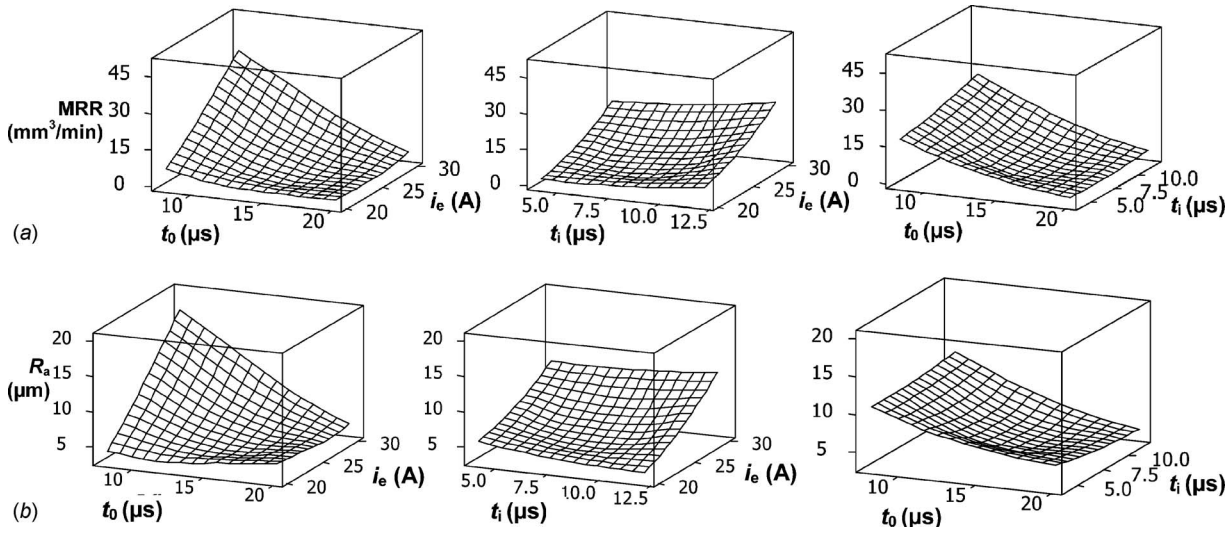

Fig. 10 Projected surfaces of (*a*) MRR and (*b*) R_a versus i_e and t_0, i_e and t_i, and t_i and t_0 for roughing EDM

was improved from 2.5 μm to 0.8 μm R_a by reducing the discharge current from 20 A to 1 A. The reduced discharge current lowered the discharge energy per pulse and generated finer craters and lower surface roughness. However, the MRR also dropped quickly, from 0.81 mm^3/min to 0.13 mm^3/min.

4.4 Gas Pressure. The effect of the gas pressure input to the spray generator on surface finish and MRR in near-dry EDM finishing with graphite electrode and kerosene-air mixture is shown in Fig. 9. As seen in the figure, the surface roughness is nearly unaffected. Under the stable discharge conditions, the surface roughness mostly depends on the discharge energy. The MRR gradually increases until the gas pressure reaches 480 kPa. The enhanced gas flow provided better debris flushing as well as more oxygen content. In the following DOE of the finishing EDM, the gas pressure was set at 480 kPa.

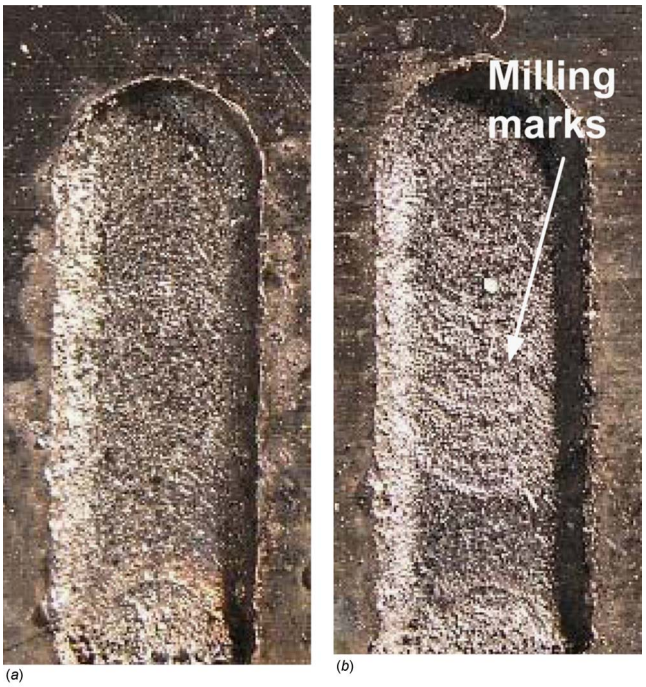

Fig. 11 Optimal micrographs of EDM surfaces at normal discharge mode: (*a*) Without milling mark, R_a=4.32 μm (i_e=20 A, t_i=12 μs, t_0=8 μs, u_e=40 V, and u_i=160 V) and (*b*) with milling mark, R_a=6.13 μm (i_e=20 A, t_i=4 μs, t_0=20 μs, u_e=80 V, and u_i=260 V)

4.5 Abnormal Discharges and Explosion Mode. For roughing EDM, at certain discharge parameter settings of high discharge energy input, i.e., high i_e, high t_i, and low t_0, the discharge may occur in the explosion mode [4] with uncontrollable material removal and excessive electrode wear. An upper limit of discharge energy input is applied for dry EDM with an oxygen medium.

5 Experiment III Results: Design of Experiments

5.1 Roughing Design of Experiments. The DOE results for oxygen assisted dry EDM roughing are summarized in Table 4. The ANOVA indicates that the significant terms influencing the MRR are t_i, i_e, and t_0, and the second order interaction, $i_e^* t_0$. The t_i and i_e are commonly recognized important EDM process parameters because they determine the discharge energy. The significance of t_0 is consistent with Kunieda et al. [4], who reported that by maintaining t_0 in the range of 5–10 μs, the discharge was under the "quasiexplosion mode" and the MRR was considerably increased compared with that at longer t_0. In the high energy EDM setup of this study, a t_0 lower than 5 μs induced the "explosion mode," resulting in abnormal discharge, deteriorated machined surface, and excess electrode wear.

The projected surfaces of MRR and surface roughness versus t_i, i_e, and t_0 are shown in Figs. 10(*a*) and 10(*b*), respectively. In the first plot of Fig. 10(*a*), a very steep rise of MRR is observed when increasing i_e and decreasing t_0. It indicates that both high i_e (>30 A) and low t_0 (<8 μs) are required to promote the intense MRR mode in dry EDM with oxygen. In the study of Kunieda et al. [4], all experiments were conducted at i_e=40 A, and hence only the significance of t_0 on the discharge mode was noticed. In this experiment, the effect of i_e is also addressed. The high discharge energy input via high i_e and high discharge frequency as a result of low t_0 stimulates the rapid exothermal oxidation and generates a large amount of heat. As a result of the intensified heat, the MRR is dramatically increased.

The main factors, i_e and t_0, and second order interactions, $i_e^* t_0$, $i_e^* t_i$, and $t_i^* t_0$, are found to be the significant terms influencing the R_a value. Figure 10(*b*) shows the effect of the significant terms on the surface finish. Generally, lower i_e and higher t_0 yield a better surface finish. The effect of t_i on the surface finish is complicated. In the last two plots of Fig. 10(*b*), at high i_e or low t_0 (high MRR),

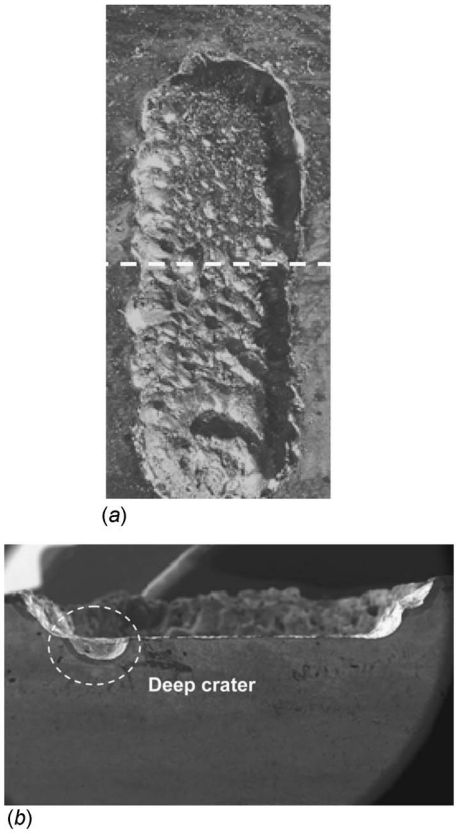

Fig. 12 Optical micrographs of the quasiexplosion mode EDM surface with deep craters (*a*) top view and (*b*) cross section view (i_e=30 A, t_i=12 μs, t_0=8 μs, u_e=60 V, and u_i=260 V)

higher t_i increases the surface roughness. However, at low i_e or high t_0 (low MRR), reducing t_i unexpectedly increases the surface roughness. As shown in the enlarged pictures of the EDM surface at a normal discharge mode in Fig. 11, at low t_i (=4 μs), milling marks can be observed on the machined surface. At low t_i, low i_e, and high t_0, the energy input is small and not appropriate for a large depth of cut. The material removal was not efficient and the electrode feeding was slow with frequent electrode retraction, which caused the milling marks. This explains why the surface roughness cannot be improved though the MRR has been reduced at low t_i.

At extremely high i_e and low t_0, the surface roughness was high, exceeding 18 μm R_a. Figure 12 shows the optical micrographs of the surface after quasiexplosion mode EDM. Deep craters as a result of arcing or energy concentration caused by rapid oxidation can be observed. These deep craters severely deteriorated the surface quality.

5.2 Finishing Design of Experiments. The MRR and surface roughness results for near-dry EDM finishing DOE using water-nitrogen medium and graphite electrode are summarized in Table 5. According to ANOVA, the significant terms influencing the MRR are the main factors, i_e and t_i, and second order interaction, $t_0 {}^{*} t_i$.

The projected surfaces of MRR versus t_i, i_e, and t_0 are shown in Fig. 13(*a*). High i_e and t_i increases MRR. The effect of t_0 varies with the level of t_i. At high t_i, the MRR decreases when decreasing t_0. Higher t_i generates more debris and requires longer t_0 to recondition the discharge gap. Otherwise, by reduced t_0, arcing tends to occur due to the degraded discharge gap condition, the electrode frequently retracts, and the MRR decreases. The degraded discharge gap condition also deteriorated the surface finish. At low t_i, less debris was generated with lower discharge energy. Less time is required to recondition the discharge gap. In this case, shorter t_0 increased the discharge frequency and therefore increased the MRR.

It is found that the main factors, i_e, t_i, and t_0, and second order interaction, $t_0 {}^{*} t_i$, have significant effects on the surface finish. The projected surfaces of surface roughness versus t_i, i_e, and t_0 are shown in Fig. 13(*b*). The second plot of the figure shows that the surface finish can be efficiently improved by decreasing i_e and t_i. Similar to the MRR results, the effect of t_0 varies with the level of t_i. At high t_i, the surface finish deteriorates with decreasing t_0 due to the arcing in the degraded discharge gap condition. Under low t_i, a long t_0 was not required to maintain a good discharge gap condition. The surface finish is only related to the pulse discharge energy.

Generally, a linear decreasing trend of R_a is identified by reducing i_e and t_i and raising t_0. The linear trend indicates that the current machining conditions are still far from the minimum R_a region. The surface finish can be improved by reducing the discharge energy. It is also suggested by the ANOVA regression model that the steepest descent direction of R_a reduces 2 units of t_i and 1 unit of i_e and increases 0.1 units of t_0, such that the surface finish can be most efficiently improved. In the future, experiments conducted along this suggested direction are anticipated to further improve the surface finish in near-dry EDM.

6 Concluding Remarks

This research presented the high MRR dry EDM and fine surface finish near-dry EDM milling processes. Oxygen demonstrated the capability to promote MRR and exothermal oxidation in both the dry and the near-dry EDM. In oxygen assisted dry EDM, high i_e and low t_0 were found able to significantly increase the MRR.

Near-dry EDM was proven beneficial for the finishing operation. Liquid phase dispersed in the gas medium is hypothesized to enhance the electric field and thus results in a large discharge gap distance and a stable discharge at low energy input. Nitrogen and helium gases could prevent the electrolysis and yield better surface finish in near-dry EDM. Reducing the discharge energy input by reducing i_e, reducing t_i, and increasing t_0 is the key to further reduce the surface finish in near-dry finishing EDM.

Table 5 MRR and R_a results for finishing DOE

Run	1	2	3	4	5	6	7	8	9	10
MRR (mm^3/min)	0.075	0.145	0.161	0.157	0.129	0.161	0.168	0.206	0.151	0.152
R_a (μm)	0.80	1.34	1.03	1.64	0.85	1.24	1.08	1.52	1.76	1.08
Run	11	12	13	14	15	16	17	18	19	20
MRR (mm^3/min)	0.121	0.125	0.176	0.145	0.147	0.120	0.126	0.129	0.135	0.136
R_a (μm)	1.45	0.86	1.50	0.93	1.18	0.86	1.12	1.17	1.22	1.30

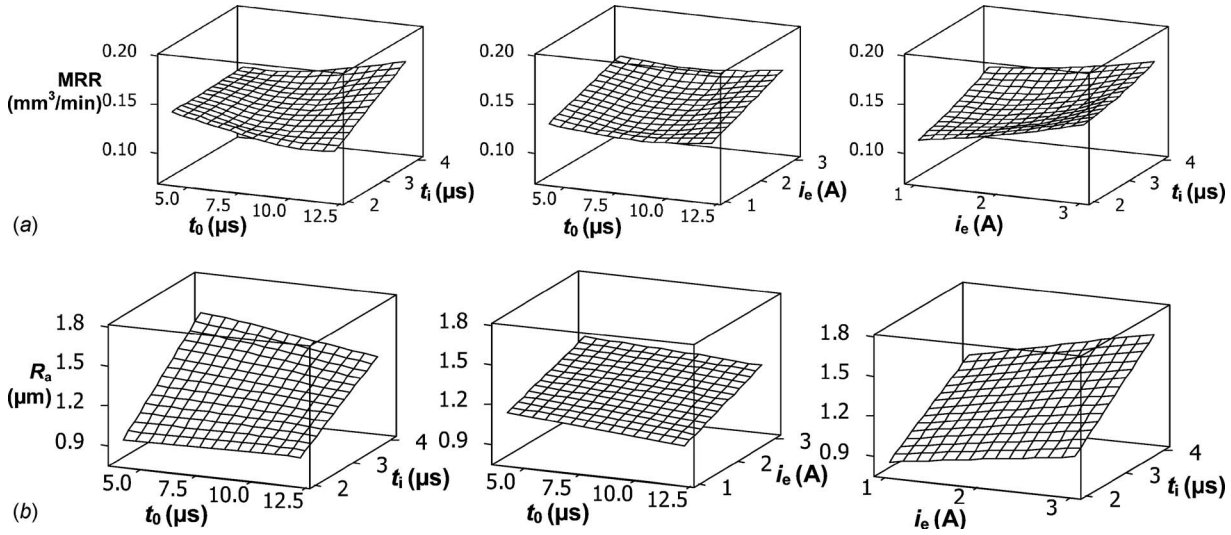

Fig. 13 Projected surfaces of (*a*) MRR and (*b*) R_a versus t_i and t_0, i_e and t_0, and i_e and t_i for finishing EDM

Future research is focused on the development of near-dry EDM with low discharge energy to generate a very fine surface finish. The machined surface and subsurface properties, such as microstructure, microhardness, residual stress, and material composition, will be investigated to characterize the near-dry EDM finishing process. The potential of forming a nitride layer for surface hardness [20] will be further tested using the liquid and/or gas with nitrogen content.

Acknowledgment

This research is sponsored by the NIST Advanced Technology Program. Discussions with Dr. Yuefeng Luo of Federal Mogul, Prof. Wanshen Zhao of Shanghai Jiao Tong University, John MacGregor of Ann Arbor Machine Co., and Prof. Masanori Kunieda and Prof. Wataru Natsu of Tokyo University of Agriculture and Technology are greatly appreciated.

References

[1] NASA, 1984, "Inert-Gas Electrical-Discharge Machining," NASA Technical Brief No. NPO-15660.
[2] Kunieda, M., and Yoshida, M., 1997, "Electrical Discharge Machining in Gas," CIRP Ann., **46**(1), pp. 143–146.
[3] Kunieda, M., and Furudate, C., 2001, "High Precision Finish Cutting by Dry WEDM," CIRP Ann., **50**(1), pp. 121–124.
[4] Kunieda, M., Miyoshi, Y., Takaya, T., Nakajima, N., Yu, Z. B., and Yoshida, M., 2003, "High Speed 3D Milling by Dry EDM," CIRP Ann., **52**(1), pp. 147–150.
[5] Kao, C. C., Tao, J., Lee, S. W., and Shih, A. J., 2006, "Dry Wire Electrical Discharge Machining of Thin Workpiece," Trans. NAMRI/SME, **34**, pp. 253–260.
[6] Tanimura, T., Isuzugawa, K., Fujita, I., Iwamoto, A., and Kamitani, T., 1989, "Development of EDM in the Mist," *Proceedings of Ninth International Symposium of Electro Machining (ISEM IX)*, Nagoya, Japan, pp. 313–316.
[7] Kao, C. C., Tao, J., and Shih, A. J., 2007, "Near Dry Electrical Discharge Machining," Int. J. Mach. Tools Manuf., **47**(15), pp. 2273–2281.
[8] Kunieda, M., Lauwers, B., Rajurkar, K. P., and Schumacher, B. M., 2005, "Advancing EDM Through Fundamental Insight Into the Process," CIRP Ann., **54**(2), pp. 599–622.
[9] Shugg, W. T., 1986, *Handbook of Electrical and Electronic Insulating Materials*, Van Nostrand Reinhold, New York, pp. 230–234.
[10] Yaws, C. L., 1995, *Handbook of Transport Property Data: Viscosity, Thermal Conductivity, and Diffusion Coefficients of Liquids and Gases*, Gulf, Houston, TX, pp. 192–193.
[11] Avallone, E. A., and Baumeister, T., 1996, *Standard Handbook for Mechanical Engineers*, 10th ed., McGraw-Hill, New York, pp. 4–82.
[12] Vedensky, B. A., and Vul, B. M., 1965, *Encyclopedia Dictionary in Physics 4*, Soviet Encyclopedia, Moscow, p. 240.
[13] Gerasimov, A. I., 2005, "Water as an Insulator in Pulsed Facilities," Instrum. Exp. Tech., **48**(2), pp. 141–167.
[14] Peyton, K. B., 2002, *Ondeo/Nalco Fuel Field Manual*, McGraw-Hill, New York, p. 112.
[15] Forsythe, W. E., 2003, *Smithsonian Physical Tables*, Knovel, Norwich, NY, p. 322.
[16] Incropera, F. P., and DeWitt, D. P., 2007, *Introduction to Heat Transfer*, 5th ed., Wiley, Hoboken, NJ, pp. 102–111.
[17] Yang, D. Y., and Cao, F. G., 2007, "The Development of Mirror Machining in EDM Sinking Process," *Proceedings of 15th International Symposium of Electro Machining (ISEM XV)*, Industrial and Management Systems Engineering, Pittsburgh, PA, pp. 57–62.
[18] Hockenberry, T. O., and Williams, E. M., 1967, "Dynamic Evolution of Events Accompanying the Low-Voltage Discharge Employed in EDM," IEEE Trans. Ind. Gen. Appl., **3**(4), pp. 302–309.
[19] Koenig, W., Wertheim, R., Zvirin, Y., and Toren, M., 1975, "Material Removal and Energy Distribution in Electrical Discharge Machining," CIRP Ann., **24**(1), pp. 95–100.
[20] Yan, B. H., Tsai, H. C., and Huang, F. Y., 2005, "The Effect in EDM of a Dielectric of a Urea Solution in Water on Modifying the Surface of Titanium," Int. J. Mach. Tools Manuf., **45**(2), pp. 194–200.
[21] Kunieda, M., and Furuoya, S., 1991, "Improvement of EDM Efficiency by Supplying Oxygen Gas Into Gap," CIRP Ann., **40**(1), pp. 215–218.
[22] Carrano, A. L., Mehta, B., and Low, J. C., 2004, "Response Surface Methodology of Die-Sink Electro-Discharge Machined Surfaces," *IIE Annual Conference and Exhibition, Institute of Industrial Engineers*, Houston, TX, pp. 787–792.
[23] Luis, C. J., Puertas, I., and Villa, G., 2005, "Material Removal Rate and Electrode Wear Study on the EDM of Silicon Carbide," J. Mater. Process. Technol., **164–165**(15), pp. 889–896.
[24] Puertas, I., Luis, C. J., and Villa, G., 2005, "Spacing Roughness Parameters Study on the EDM of Silicon Carbide," J. Mater. Process. Technol., **164–165**(15), pp. 1590–1596.
[25] Luo, Y. F., 1997, "Dependence of Interspace Discharge Transitivity Upon the Gap Debris in Precision Electrodischarge Machining," J. Mater. Process. Technol., **68**(2), pp. 121–131.
[26] Luo, Y. F., and Chen, C. G., 1990, "Effect of a Pulsed Electromagnetic Field on the Surface Roughness in Superfinishing EDM," Precis. Eng., **12**(2), pp. 97–100.
[27] Schumacher, B. M., 1987, "EDM Technology for Precision Workpieces With Excellent Surface Quality," *Proceedings of the 7th International Symposium of Electro Machining (ISEM VII)*, IFS Ltd., Birmingham, UK, pp. 124–135.